Zero-Field Nuclear Magnetic Resonance of Ordered $RbNiF_3$

George H. Stauss
Naval Research Laboratory, Washington, D. C. 20390
(Received 5 June 1970)

NMR spectra of ^{19}F and ^{61}Ni have been obtained at 4.2 °K, in zero external field, by a spin-echo study of hexagonal ferrimagnetic $RbNiF_3$. The two inequivalent F sites yield broad spectra, strongly peaked at the extremes, characteristic of random magnetization orientations confined to the c plane. The extremes of the higher-frequency h-site spectrum occur at 103 ± 1 and 227 ± 1 MHz; of the lower-frequency k site, at 5.7 ± 0.2 and 19.6 ± 0.2 MHz. Comparison of the F hyperfine coupling constants indicates that at 4.2 °K both the isotropic and pseudodipolar parts are reduced by roughly 10% with respect to the room-temperature values obtained by Smolenskii *et al.* for the paramagnetic phase. The ^{61}Ni spectra are sharp quadrupole triplets, with the center frequency of the more populous f site of 17.06 ± 0.01, of the a site at 18.30 ± 0.01 MHz, in agreement with expectation for Ni^{2+} ions. The quadrupole splitting parameters e^2qQ/h are 1.54 and 0.68 MHz, respectively.

I. INTRODUCTION

The compound $RbNiF_3$ is of particular interest within the group of ABF_3 trifluorides with nonmagnetic A and divalent magnetic B ions. While most of these materials are antiferromagnets with cubic perovskitelike structures,[1,2] $RbNiF_3$ (and also $TlNiF_3$)[3] assumes the hexagonal $BaTiO_3$ form and below 139 °K is a ferrimagnet.[1,4] Furthermore, it is transparent to visible light. Optical,[1,5–7] magnetic,[1,4,8] and ferromagnetic resonance[9,10] studies have been made in the magnetically ordered material, but the only nuclear-magnetic-resonance (NMR) work so far reported has been the careful single-crystal work of Smolenskii *et al.*[11] done in the paramagnetic region with the ^{19}F resonances.

This paper describes the results of zero-field spin-echo NMR studies of the ordered state of $RbNiF_3$ at 4.2 °K. Resonance spectra were obtained for ^{61}Ni as well as for ^{19}F nuclei, in each type of lattice site. The ^{19}F spectral shapes are examples of the uncommon powder average pattern corresponding to a random distribution of magnetization orientations within a plane. The isotropic and anisotropic hyperfine coupling parameters describing the ^{19}F spectra are in general agreement with the NMR results from the paramagnet, but indicate that there is a significant temperature dependence to these parameters. The sharp ^{61}Ni resonances occur at frequencies compatible with core polarization plus orbital fields for Ni^{2+} ions. The measured quadrupolar splittings, on the other hand, are smaller than expected and suggest structural changes with cooling.

II. EXPERIMENT

The sample used was a collection of small crystals (≥ 0.5 mm diam) made by Becker following the $RbF + NiCl_2$ method described by Smolenskii *et al.*[4] No second phase was detectable by x-ray examination. Agreement with the x-ray spectrum given by Rüdorff *et al.*[2] was excellent.

Resonance spectra were obtained by the usual spin-echo techniques, using a cold-finger Dewar to contain the sample. Since a broad range of frequencies was covered, several circuit configurations were employed. At frequencies below 200 MHz, an external tuned circuit driven by a pulsed oscillator was used. Above this frequency, the sample was inserted directly into the tuning element of a lecher-line oscillator. It was found that a great amount of rf enhancement, with a maximum value in excess of 10^4, occurs in this material. In order to obtain reliable spectra it was thus necessary to control the rf field amplitude carefully and to keep to very low amplitudes. It was this enhancement which permitted observation of the resonances at all; application of external fields weakened the resonances below observable levels, due to removal of domain walls, before any field shifts could be detected. The absolute signs of the hyperfine fields therefore could not be determined directly.

Part of the $RbNiF_3$ structure is illustrated in Fig. 1. Ni atoms are found in two inequivalent positions, with twice as many in f as in a sites. Their surrounding F neighbors form octahedra, more distorted about f positions than about a. The F atoms occur two-thirds in k sites, with the rest in inequivalent h sites. The two Ni sublattices align antiparallel in the ordered state, with the easy direction of magnetization perpendicular to the unique c axis. The axial anisotropy field is of the order of 30 kOe, whereas almost no anisotropy is observed within the c plane.[1,4,9]

The experimentally observed resonance spectra of $^{19}F(k)$ and $^{19}F(h)$ are displayed in Figs. 2 and 3. The ^{61}Ni lines occur within the spectrum shown in Fig. 2. The ^{19}F patterns evinced in Figs. 2 and 3 are characteristic of a random distribution of mag-

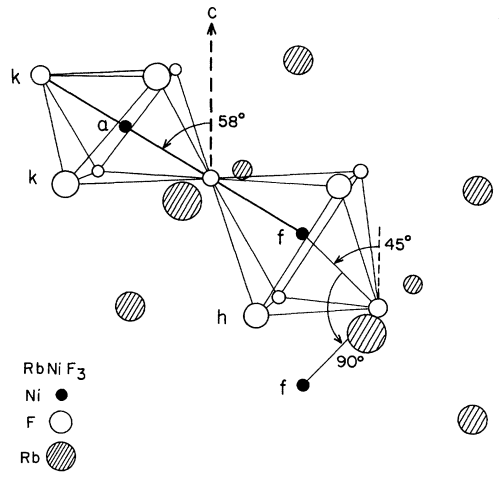

FIG. 1. Portion of the $RbNiF_3$ lattice (D_{6h}^4). $a_0 = 5.84$ Å, $c_0 = 14.31$ Å. Site symmetries: Ni($2a$) $-\bar{3}m$, Ni($4f$) $-3m$, F($6h$) $-mm$, F($12k$) $-m$.

netization directions within the c plane, an unusual pattern for a collection of irregularly shaped small particles. It is a consequence of the strong axial anisotropy which prevents a three-dimensional randomization which shape anisotropy could otherwise produce. If the parts of the hyperfine fields which depend on magnetization direction within the plane are of pseudodipolar form, retention of only the components parallel to the magnetization leads to the prediction of a symmetric doubly peaked pattern. With the inclusion of all dipolar components, as is necessary for frequency distributions of such great extent, one finds that the shape is modified, being weakened relatively at the lower-frequency peak. The theoretically obtained shape functions, the development of which is described in Sec. III, are

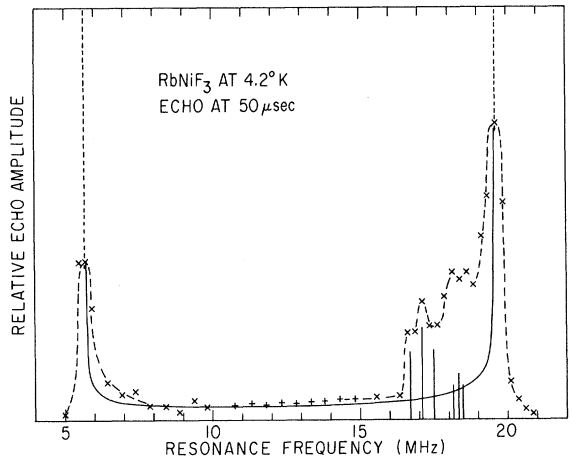

FIG. 2. Spin-echo trace of $^{19}F(k)$ spectrum with superimposed ^{61}Ni spectra.

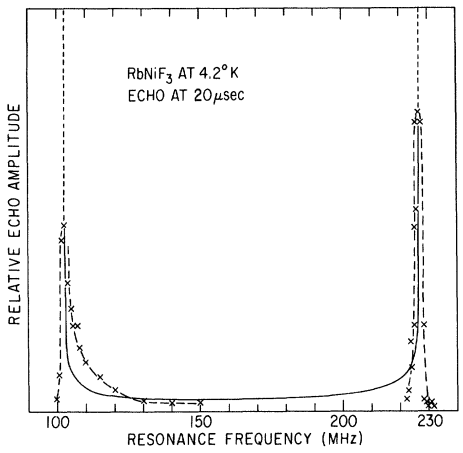

FIG. 3. Spin-echo trace of $^{19}F(h)$ spectrum.

shown in Figs. 2 and 3 as smooth curves.

The shapes shown in Figs. 2 and 3 represent composites of several overlapping regions covered by different instrumental configurations. The great differences between minimum and maximum frequencies prevented continuous tracing across the spectra. In the high-frequency trace, there was a considerable loss in sensitivity on going to the lecher-line oscillator, so that only the region near the upper peak could be observed. In both spectra, the regions of minimum amplitude were near noise level, and subject to considerable scatter.

Across the ^{19}F spectra, relaxation times were not completely uniform. In Fig. 2 the transverse time T_2 was 50 μsec at the lower peak, about half that at 10 MHz, and again 50 μsec above 15 MHz. The longitudinal time T_1, estimated roughly, increased from 0.1 sec at the low end to 1 sec at the high end. For Fig. 3, the T_2 values were about 12 μsec at both peaks, and T_1 was a few milliseconds. Since Fig. 2 was obtained with the echo 50 μsec from the initial trigger pulse, and Fig. 3 at 20 μsec, some distortion may be attributed to changes in T_2. Additional broadening results from the frequency spread of the pulses. In Fig. 3, 2-μsec pulses were employed; 1.5-μsec pulses were used below 15 MHz in Fig. 2, 5-μsec pulses above.

It was possible to examine the ^{61}Ni spectra separately, in consequence of much longer T_2 relaxation times there. These spectra are shown in Fig. 4. Given the disposition of magnetization only in the c plane, one anticipates no angular variation in the Ni resonances, since the c axis is a threefold symmetry axis for both Ni sites. This is borne out by the sharp spectra in Fig. 4. The structure here is the result of quadrupole interactions. Figure 2 shows the presence of the superimposed Ni signals. They do not match in detail the shape of Fig. 4 because in tracing the ^{19}F shape the rf pulses were somewhat

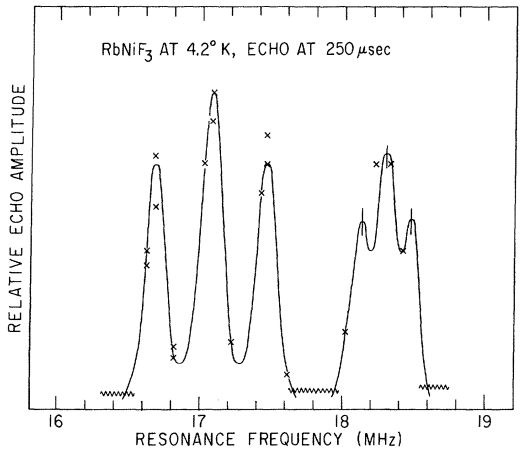

FIG. 4. Spin-echo trace of ^{61}Ni spectra with ^{19}F(k) spectrum suppressed. The high-frequency shape is sketched using the positions of the three maxima indicated by the vertical bars. These could be located by hand-sweeping the oscillator.

too short and strong so that the sharp Ni shapes were distorted and broadened.

Figure 4 was made using 5-μsec pulses and the peaks in the higher-frequency triplet located by means of 20-μsec pulses. The peak separations could also be measured by means of clear beat patterns in the echo shapes. These lines were obtained free of the ^{19}F signal by observation of the echo 250 μsec after the initial trigger. The T_2 for both ^{61}Ni sets is 750 μsec and T_1 approximately 20 msec.

Identification of the sources of the various spectra is made as follows. Figure 2 arises from k-site ^{19}F, Fig. 3 from h-site ^{19}F. These are the only nuclei not possessing threefold axial site symmetry about the c axis. As will be discussed further below, the k site, lying nearest oppositely directed a- and f-site Ni moments, will have a much smaller hyperfine field than the h site with its pair of nearest-neighbor f-site Ni's. The two triplets of Fig. 4 arise from ^{61}Ni; Rb can be eliminated because of the large magnitudes of the fields and because of the absence of ^{85}Rb-^{87}Rb spectral pairs. One identifies the higher-frequency set with a-site ^{61}Ni from its weaker intensity. Using these identifications, one thus obtains the experimental parameters given in Table I.

III. DISCUSSION

From the experimental results it is possible to identify separately, for the ^{19}F sites, the signs and magnitudes of the isotropic and pseudodipolar hyperfine fields and of the true dipolar fields. This is done by examining the structure of the spectra and by making use of the resonance information from the paramagnetic region. One can then determine the effect of reducing temperature on the hyperfine coupling constants at the ^{19}F sites. The signs of the hyperfine fields and an estimate of the size of the nuclear quadrupole moment of ^{61}Ni will also be extracted from the data.

^{19}F

Considering first the ^{19}F data, we note that in the analysis of the ^{19}F NMR in the paramagnetic region, Smolenskii *et al.* [11] found that all of their results could be described in terms of local groups each composed of an F atom and its two nearest Ni neighbors. (See Fig. 1.) The effects of the Ni are further limited to isotropic and point dipolelike terms. With the exception of fairly small dipolar contributions from farther neighbors not conforming to the geometry of these systems, this model is adequate to discuss the present problem as well. It is necessary to consider the entire dipole field, however, rather than the component parallel to the magnetization, as was sufficient for the paramagnet.

With a dipole $\vec{\mu}$ at a Ni(i) atom position ($i = a$ or f), located in the direction $(\pm \sin\theta_{ij}, 0, \cos\theta_{ij})$ from an F(j) atom ($j = h$ or k) in a rectangular coordinate system with z along the c axis, the dipole field on the F(j) nucleus takes the form $\vec{H} = P_{ij}\overleftrightarrow{T}\cdot\hat{\mu}$, where the tensor $\overleftrightarrow{T}$ is given by

$$\begin{vmatrix} 3\sin^2\theta_{ij} - 1 & 0 & \pm 3\sin\theta_{ij}\cos\theta_{ij} \\ 0 & -1 & 0 \\ \pm 3\sin\theta_{ij}\cos\theta_{ij} & 0 & 3\cos^2\theta_{ij} - 1 \end{vmatrix} .$$

The coefficient P_{ij} contains a dipolar part $|\mu|/r_{ij}^3$ and a hyperfine field term $-(1/\gamma\hbar)A_p(ij)\langle S_M\rangle_i$ where $\langle S_M\rangle_i$ is the expectation value of the Ni(i) spin in the magnetization direction. Here γ is the nuclear gyromagnetic ratio. There is, in addition, an isotropic (uniform) field contribution $U_{ij}\hat{\mu}$, where $U_{ij} = -(1/\gamma\hbar) \times A_u(ij)\langle S_M\rangle_i$. In the above, $\hat{\mu}$ denotes a unit vector.

Immediately limiting the discussion to a magnetization direction $(\cos\varphi, \sin\varphi, 0)$ confined to the c plane, the effective field at the F(j) nucleus becomes

$$\vec{H}(j) = \{[U_{ij} + P_{ij}(3\sin^2\theta_{ij} - 1)]\cos\varphi,\ (U_{ij} - P_{ij}) \times \sin\varphi,\ 3P_{ij}\sin\theta_{ij}\cos\theta_{ij}\cos\varphi\}.$$

At an F(h) site there are two Ni(f) neighbors giving the same U_{fh} and P_{fh} coefficients and with positions $[-\sin\theta_{fh}, 0, \cos(\theta_{fh}$ or $\pi - \theta_{fh})]$. At the F(k) site, the coefficients U_{fk}, U_{ak} and P_{fk}, P_{ak} are unequal for the Ni(f) and Ni(a) neighbors, and the positions are $[-\sin\theta_{fk}, 0, \cos(\pi - \theta_{fk})]$ and $(\sin\theta_{ak}, 0, \cos\theta_{ak})$. The analysis by Smolenskii *et al.*, [11] however, led to

TABLE I. Experimental parameters (MHz).

^{19}F(k)	$\nu_{min} = 5.7 \pm 0.2$	$\nu_{max} = 19.6 \pm 0.2$
^{19}F(h)	$\nu_{min} = 103 \pm 1$	$\nu_{max} = 227 \pm 1$
^{61}Ni(a)	$\nu_{ctr} = 18.30 \pm 0.01$	$e^2qQ/h = 0.68 \pm 0.02$
^{61}Ni(f)	$\nu_{ctr} = 17.06 \pm 0.01$	$e^2qQ/h = 1.54 \pm 0.02$

the satisfactory assumption that $\theta_{fk} = \theta_{ak} \equiv \theta_k$. Thus, combining the effects of the two neighbors, with $\theta_h \equiv \theta_{fh}$, $U_h \equiv 2U_{fh}$, $P_h \equiv 2P_{fh}$, $U_k \equiv U_{fk} + U_{ak}$, and $P_k \equiv P_{fk} + P_{ak}$, one can write

$$\vec{H}(h) = \{[U_h + P_h\ (3\sin^2\theta_h - 1)]\cos\varphi,$$
$$(U_h - P_h)\sin\varphi,\ 0\},$$
$$\vec{H}(k) = \{[U_k + P_k\ (3\sin^2\theta_k - 1)]\cos\varphi,$$
$$(U_k - P_k)\sin\varphi,\ 3P_k \sin\theta_k \cos\theta_k \cos\varphi\}.$$

Hence

$$H^2(h) = (U_h - P_h)^2 + [6U_hP_h \sin^2\theta_h + 3P_h^2 \sin^2\theta_h\ (3\sin^2\theta_h - 2)]\cos^2\varphi,$$
$$H^2(k) = (U_k - P_k)^2 + 3P_k\ (2U_k + P_k)\sin^2\theta_k \cos^2\varphi.$$

The theoretical shapes drawn in Figs. 2 and 3 were made on the assumption that there is a uniform distribution in azimuthal angle φ; the shape functions are thus of the form $N(H) = 2H/(d/d\varphi)\,H^2$. The peaks of this function in both cases occur at $\cos^2\varphi = 0$ and 1, which place the positions of the peaks at

$$H^2(h) = (U_h - P_h)^2 \text{ or } (U_h - P_h + 3P_h \sin^2\theta_h)^2,$$
$$H^2(k) = (U_k - P_k)^2 \text{ or } (U_k - P_k)^2 + 3\sin^2\theta_k\ (P_k^2 + 2U_kP_k).$$

It turns out that $U_k - P_k$ must be the lower-frequency peak of $H(k)$ if the ratio of lower to higher frequency is less than $\cos\theta_k$. This is the case for the quoted value,[11] $\theta_k = 58° \pm 2°$. With this limitation, two pairs of solutions (U_k, P_k) are possible. U_k and P_k have the same signs but absolute sign is not determined by the solutions. Similarly, for $H(h)$, where $\theta_h = 45° \pm 2°$, the absolute signs are not determined by the data. Here $U_h - P_h$ can represent either peak, so there are four possible sets of solutions.

To select the proper signs and solutions, we return to the paramagnetic results. We look for the results most compatible with the room-temperature data, and for this purpose evaluate the quantities U_j and P_j predicted by the parameters of Smolenskii *et al.* Applying the hyperfine coupling constants A for 300 °K (cf. Table III below) to low temperatures in the ordered system, where $\langle S_M \rangle_f = -1$ and $\langle S_M \rangle_a = +1$ for the Ni^{2+} ions, one obtains the predicted U_j and P_j values given in Table II. Included here is the contribution from eight nearest Ni moments; the dipole field tensor is roughly proportional to that of the two nearest-neighbor Ni(f)'s and leads to P_h (dipolar) = +5.25 kOe. There is very nearly cancellation of both hyperfine and dipolar contributions to P_k; uncertainties in the structure parameters allow no more definite evaluation of the dipole sum.

Comparing these results to the low-temperature experimental values, the proper choice of F(h) values is made easily. The signs on the F(h) sites will not change upon ordering; these were observed[11] both to be positive with respect to the Ni(f) polarization, which becomes the direction of spontaneous magnetization. One also expects all field contributions to scale together almost exactly at the F(h) site, and on this basis the solution entered in Table II is to be preferred. The error limits shown include both measurement uncertainties and the error in θ_h.

The choice of solution is less direct for the F(k) sites. However, one expects P_k to be significantly smaller than the predicted value of U_k; this and the better agreement with the paramagnetic results select the solution shown in Table II. The errors include the uncertainty in θ_k. In this case, however, as will be discussed below, considerations of farther-neighbor dipoles will increase the range of error.

The solution for the F(k) parameters is based on the geometry of the nearest-neighbor positions alone. Since the cancellation of terms is almost complete, modifications introduced by farther neighbors can be of relatively great importance. In order to evaluate the proper dipole field one must know the lattice structural parameters in detail. The four parameters necessary to describe the Ni- and F-site positions in this space group are related to the values of θ_h and θ_k; one obtains for them the relationships $u_f = 0.853 \pm 0.012$, $u_h = 0.521 \pm 0.028$, and $u_k = 1 - (2.27 \pm 0.20)v_k$. With these values, and taking as an example the values $u_k = 0.84$ and $v_k = 0.07$ near those for $BaTiO_3$, one finds that about half of the observed P_k value is attributable to dipolar fields; in this case fields from more distant neighbors are significant and their inclusion alters the geometry of the system. Recast in this way, the isotropic field value U_k is reduced by about 0.25 kOe in magnitude from Table II.

It is apparent that within the errors quoted, the low-temperature and room-temperature results are in agreement. On the other hand, the agreement is at the limits of error, and the paramagnetic results consistently overestimate the low-temperature hyperfine fields. This suggests that the hyperfine coupling constants actually are reduced in going from

TABLE II. Hyperfine fields (kOe). Signs with respect to magnetization direction.

	Observed		Predicted[a]	
^{61}Ni(a)	$H_{hf} = +48.22 \pm 0.03$			
^{61}Ni(f)	$H_{hf} = -44.95 \pm 0.03$			
	U	P	U	P
^{19}F(h)	$+46.4 \pm 2$	$+20.7 \pm 2$	$+50.5 \pm 3$	$+23.3 \pm 1.8$
^{19}F(k)	-2.85 ± 0.1	-1.42 ± 0.08	-5.27 ± 3	≈ 0

[a]Reference 11. See text.

room temperature to 4.2 °K. The comparison between the hyperfine coupling constants obtained here and at room temperature is shown in Table III.

TABLE III. Hyperfine coupling constants (10^{-19} erg).

	4.2 °K	Room temperature[a]
$A_u(fh)$	6.2 ± 0.3	6.7 ± 0.4
$A_p(fh)$	2.1 ± 0.3	2.4 ± 0.2
$A_u(fk) - A_u(ak)$	-0.7 ± 0.1	-1.4 ± 0.8
$A_p(fk) - A_p(ak)$	≈ -0.2	≈ 0

[a]Reference 11.

^{61}Ni

We turn now to the ^{61}Ni results. In the spectra of ^{61}Ni, one observes discrete hyperfine fields, with quadrupolar splitting. The effective field values represent combinations of isotropic hyperfine fields with true and pseudodipolar fields which are independent of orientation within the c plane. One calculates the point dipolar contributibution to be -0.79 kOe at f sites and $+0.17$ kOe at a sites, with respect to the magnetization direction. These are small perturbations in the face of the large terms giving the total fields.

An examination of Ni^{2+} hyperfine fields by Locher and Geschwind[12] found a value of -254 kOe owing to core polarization effects. (The sign refers to the direction of the ionic moments.) To this must be added a contribution of $+125 \langle r^{-3} \rangle \Delta g |S|$ kOe owing to unquenched orbital angular momentum.[12,13] Here the radial integral is to be expressed in atomic units; evaluation gives[14] 7.09 a.u. The quantity $\Delta g = g - 2$ refers to the effective spectroscopic splitting factor observed in the magnetization direction. From the saturation moment normal to the c axis,[1] one obtains $g_\perp = 2.24$. In the present case, with the moments confined to the c plane, this leads to an orbital hyperfine field of +212 kOe. Assuming the g values are similar at both a and f sites, one thus finds the total fields at both to be -42 kOe. The observed field values are in good agreement with prediction, indicating that the signs of the fields with respect to the magnetization [Ni(f) moment direction] are as summarized in Table II.

The splitting between the two sites is opposite to that expected from the true dipole fields. Thus the parts of the hyperfine coupling effects which oppose the core polarization are greater at f sites than at a sites by 3.9 kOe. This difference corresponds to a 2% greater $\Delta g_\perp$, but could arise from several sources related to the different environments of the two sites.

The spectra of Fig. 4 represent one of the few cases in which ^{61}Ni quadrupole splitting has been distinctly resolved, with the values of e^2qQ/h shown in Table I. With the reasonable assumption that intra-ionic field gradients from the unfilled $3d$ shell can be ignored for the orbital singlet ground state of the $3d^8$ configuration,[13] one has the effective electrostatic field gradient $eq = (eq)_{\text{lattice}}(1 - \gamma_\infty)$, taking into account the Sternheimer antishielding factor. Point-charge estimates of the values of $(eq)_{\text{lattice}}$, made with the structure parameters mentioned earlier, are quite different for the two sites. In conjunction with the reported ^{61}Ni quadrupole moment[15] and a Sternheimer factor[16] of about 10, these values predict splittings considerably greater than those observed. The values of $(eq)_{\text{lattice}}$ are very sensitive to the structure parameters and may further be modified by covalent charge transfer, so that detailed comparisons cannot be made. However, a consistent improvement in the calculated values results if the distortion of the F octahedra is less here than at room temperature.

IV. SUMMARY

The present work with $RbNiF_3$ confirms in general the room-temperature results of Smolenskii *et al.*[11] for the ^{19}F hyperfine interactions. It further indicates a temperature dependence or an influence of magnetic ordering on the coupling parameters. The unusual two-dimensional distribution of magnetization directions and the high rf enhancement observed, for nuclei undoubtedly situated within domain walls, are further signs of extremely small magnetic anisotropy within the c plane.

The positions of the ^{61}Ni resonances are in agreement with the expected behavior for Ni^{2+} ions and demonstrate that between the two inequivalent sites only a very small difference in $g_\perp$ factors exists. On the other hand, one anticipates negligible intra-ionic electrostatic field gradients for Ni^{2+}; in their absence, the observed quadrupolar splittings are inconsistent with the reported[15] quadrupole moment of ^{61}Ni, unless the room-temperature structure is modified.

ACKNOWLEDGMENT

I am grateful to R. A. Becker for preparing the sample used in this work.

[1]M. W. Shafer, T. R. McGuire, B. E. Argyle, and G. J. Fan, Appl. Phys. Letters 10, 202 (1967).

[2]W. Rüdorff, J. Kändler, and D. Babel, Z. Anorg. Allgem. Chem. 317, 261 (1962).

[3]K. Kohn, R. Fukuda, and S. Iida, J. Phys. Soc. Japan 22, 333 (1967).

[4]G. A. Smolenskii, V. M. Yudin, P. P. Syrnikov, and A. B. Sherman, Fiz. Tverd. Tela 8, 2965 (1966) [Soviet Phys. Solid State 8, 2368 (1967)].

[5]S. R. Chinn and H. J. Zeiger, Phys. Rev. Letters

21, 1589 (1968).
[6]J. Tylicki, W. M. Yen, J. P. van der Ziel, and H. J. Guggenheim, Phys. Rev. 187, 758 (1969).
[7]P. A. Fleury, J. M. Worlock, and H. J. Guggenheim, Phys. Rev. 185, 738 (1969).
[8]M. P. Petrov, V. V. Moskalev, and G. A. Smolenskii, Solid State Commun. 8, 157 (1970).
[9]E. I. Golovenchits, V. A. Sanina, and A. G. Gurevich, Fiz. Tverd. Tela 10, 2956 (1968) [Soviet Phys. Solid State 10, 2334 (1969)].
[10]M. P. Petrov and S. A. Kizhaev, Fiz. Tverd. Tela 11, 2435 (1969) [Soviet Phys. Solid State 11, 1968 (1970)].
[11]G. A. Smolenskii, M. P. Petrov, V. V. Moskalev, V. S. L'vov, V. S. Kasperovich, and E. V. Zhirnova, Fiz. Tverd. Tela 10, 1305 (1968) [Soviet Phys. Solid State 10, 1040 (1968)].
[12]P. R. Locher and S. Geschwind, Phys. Rev. Letters 11, 333 (1963).
[13]A. Abragam and M. H. L. Pryce, Proc. Roy. Soc. (London) A205, 135 (1951).
[14]A. J. Freeman and R. E. Watson, in *Magnetism IIA*, edited by G. T. Rado and H. Suhl (Academic, New York, 1965), p. 167.
[15]W. J. Childs and L. S. Goodman, Phys. Rev. 170, 136 (1968).
[16]R. M. Sternheimer, Phys. Rev. 146, 140 (1966).

PHYSICAL REVIEW B VOLUME 2, NUMBER 9 1 NOVEMBER 1970

Mössbauer-Effect Studies of Iron-Tin Alloys

G. Trumpy and E. Both
Laboratory of Applied Physics II, Technical University of Denmark, Lyngby, Denmark

and

C. Djéga-Mariadassou and P. Lecocq
Laboratoire de Chimie Minérale, Faculté des Sciences, Orsay, France
(Received 16 March 1970)

Solid solutions *Fe*Sn and the compounds Fe_3Sn, Fe_5Sn_3, Fe_3Sn_2, FeSn, and $FeSn_2$ have been studied by the Mössbauer effect in both Fe and Sn nuclei. Also, standard x-ray diffraction and magnetization studies were performed. The magnetic hyperfine (hf) fields in the Fe and Sn components are not, in general, proportional to the magnetic moments. It is found that two simple relations containing the coordination numbers can be used within a wide range to describe the variations of these fields as a function of composition. The collected results indicate that the magnetic hf field at the iron nucleus is rather insensitive to the conduction-electron polarization in these alloys. The isomer shifts are linearly related to the number of Fe-Sn bonds in such a way that bonding reduces the electron densities at both nuclei. The bonding is covalentlike and predominantly unpolarized.

I. INTRODUCTION

The origins of the hyperfine (hf) effects in metals and alloys are, at present, only poorly understood. This is partly due to the fact that one has still not a satisfactory description of electrons in alloys or of ordered magnetic phenomena in metals and alloys. These problems may be approached through systematic experimental studies of hf effects, which, for instance, can be observed as a function of sample composition.

In the present work, we have carried out a study of hf structure, measured by means of the Mössbauer effect, on all the known different phases of the binary iron-tin alloy system. Both of these two components are in practice very useful Mössbauer nuclei in a wide temperature range, this being part of the reason for choosing such a system. Data on the alloys were also obtained by means of more conventional methods, such as magnetic-moment and Curie-point determinations and x-ray crystallography. The experimental results do in fact show certain regularities which may prove to be of some value in formulating theories on hf effects and in planning future experiments. It appears that hf magmetic fields and electron densities may be expressed as simple functions of the atom's surroundings. Some general relationships will tentatively be proposed and the physical mechanisms will be discussed.

II. EXPERIMENTAL METHODS

The known phases of the iron-tin system have been given by Hansen and Anderko,[1] and by Jannin *et al.*[2] The phase diagram is characterized by one solid solution, *Fe*Sn, and five definite intermetallic compounds, Fe_3Sn, Fe_5Sn_3, Fe_3Sn_2, FeSn, and $FeSn_2$.

Polycrystalline samples were prepared by diffusion. Known quantities of 99.9+% tin powder and 99.9+% iron powder contained in an evacuated quartz ampoule were annealed for fifteen days at the equilibrium temperature of the relevant phase. The samples of Fe_5Sn_3 were annealed for one month. Fin-